

Engineering Notes

ENGINEERING NOTES are short manuscripts describing new developments or important results of a preliminary nature. These Notes cannot exceed 6 manuscript pages and 3 figures; a page of text may be substituted for a figure and vice versa. After informal review by the editors, they may be published within a few months of the date of receipt. Style requirements are the same as for regular contributions (see inside back cover).

New Time-Domain Identification Technique

Fang-Bo Yeh* and Ciann-Dong Yang†

National Chen Kung University, Tainan, Taiwan

Introduction

A NOVEL methodology is proposed herein, to identify model parameters of vibrating structures. Mass, stiffness, and damping matrices corresponding to a lumped equivalent model of the tested structure are obtained directly from the impulse response data. Unlike the conventional approach that utilizes the modal shapes synthesis technique,^{1,2} the present identification scheme requires only a simple manipulation of the impulse response data. The dimension of the matrices involved in the computation procedure is of about the same degree-of-freedom as the structure under testing. A simulation study of a spring-mass damper system shows the high accuracy of the identification procedure. Even under the condition where the number of sampling points is limited, the present method gives a surprisingly good result.

Analysis

Assume that a large space structure (LSS) can be satisfactorily modeled by the following linear matrix differential equation:

$$M\ddot{x} + C\dot{x} + Kx = f \quad (1)$$

where x is the $n \times 1$ configuration vector of physical displacements, f the $n \times 1$ force vector, M the $n \times n$ symmetric positive-definite mass matrix, C the $n \times n$ symmetric positive-semidefinite damping matrix, and K the $n \times n$ symmetric positive-semidefinite stiffness matrix. Dots denote differentiation with respect to time.

Our objective is to identify the poorly known coefficient matrices M , C , and K . One straightforward way to do this is to measure the position, velocity, acceleration, and force at some discrete instants, and obtain enough measurement equations to estimate M , C , and K by the least-squares method. However, the measurement of acceleration, velocity, and displacement at all degrees-of-freedom poses practical difficulties. To obtain partial relief from this requirement, an orthogonal identification scheme has been proposed in Ref. 3, where the Chebyshev polynomials are used to approximate the acceleration data. In the case of impulse force excitation, a set of natural polynomials inherently exists in the expression of displacement, and on this polynomial basis it is shown here that the impulse response data and the model parameters have a very simple relation.

Taking the Laplace transform of Eq. (1) and assuming zero initial conditions gives

$$B(s)X(s) = F(s) \quad (2)$$

where

$$B(s) = Ms^2 + Cs + K \quad (3)$$

Here, s is the Laplace variable, and $F(s)$ the applied force vector, and $X(s)$ the resulting displacement vector in the Laplace domain. $B(s)$ is called the system matrix, and the transfer function matrix (TFM) $H(s)$ is defined as

$$H(s) = B(s)^{-1} \quad (4)$$

We expand $H(s)$ to a power series of s :

$$H(s) = H(0) + H(1)s^{-1} + H(2)s^{-2} + H(3)s^{-3} + \dots \quad (5)$$

where $H(i)$ are called the Markov parameters of the corresponding TFM. Since the elements of B are quadratic functions of s , we must have $H(0) = H(1) = 0$. In terms of $H(i)$, M , C , and K can be expressed as

$$M = H(2)^{-1} \quad (6a)$$

$$C = -H(2)^{-1}H(3)H(2)^{-1} \quad (6b)$$

$$K = H(2)^{-1}[H(3)H(2)^{-1}] - H(2)^{-1}H(4)H(2)^{-1} \quad (6c)$$

where $H(2)$ is invertible, since the impulse excitation guarantees that all degrees of freedom participate in the response. Taking the inverse Laplace transform of both sides of Eq. (5) yields

$$\begin{aligned} L^{-1}[H(s)] &= h(t) \\ &= H(2)t/1! + H(3)t^2/2! + H(4)t^3/3! + \dots \end{aligned} \quad (7)$$

where $h(t)$ is the impulse response matrix with the dimensions of $n \times n$. Equation (7) can be interpreted as a polynomial representation of the impulse response function using the standard basis $\{1, t, t^2, \dots\}$. If t is small enough, the high-order terms in the right-hand side of Eq. (7) can be neglected.

Consider an idealized measurement process wherein the impulse response data are measured at discrete instants, say t_1, t_2, \dots, t_m . Upon writing m measurement equations ($m > n$) identical to Eq. (7), one for each measurement time, the resulting matrix equations can be written as

$$(T_m \otimes I_{n \times n})Y = Z \quad (8)$$

where T_m is an $m \times m$ coefficient matrix:

$$T_m = \begin{bmatrix} t_1 & t_1^2/2! & \dots & t_1^m/m! \\ t_2 & t_2^2/2! & \dots & t_2^m/m! \\ \vdots & \vdots & \dots & \vdots \\ t_m & t_m^2/2! & \dots & t_m^m/m! \end{bmatrix} \quad (9)$$

Received June 23, 1986; revision received Oct. 13, 1986. Copyright © American Institute of Aeronautics and Astronautics, Inc., 1987. All rights reserved.

*Associate Professor, Institute of Aeronautics and Astronautics.

†Instructor, Department of Aeronautics and Astronautics.

The tensor product or the Kronecker product is denoted by \otimes , and $T_m \otimes I_{n \times n}$ means that every entry of T_m is multiplied by the identity matrix $I_{n \times n}$.

Y is an $mn \times n$ matrix containing the unknown Markov parameters:

$$Y = [H^T(2)H^T(3)...H^T(m+1)]^T \tag{10}$$

Z is an $mn \times n$ matrix containing the impulse response data:

$$Z = [h^T(t_1)h^T(t_2)...h^T(t_m)]^T \tag{11}$$

It can be shown by the properties of the Kronecker product that

$$(T_m \otimes I_{n \times n})^{-1} = T_m^{-1} \otimes I_{n \times n}$$

Thus

$$Y = (T_m^{-1} \otimes I_{n \times n})Z \tag{12}$$

Substituting $H(2)$, $H(3)$, and $H(4)$ from the solution of Eq. (8) into Eq. (6) yields the estimated model parameters M , C , and K .

One of the remarkable properties of the present method is that an increase in the number of sampling data (m) does not necessarily guarantee an improvement in the accuracy of the results. To get a fast convergent rate of Eq. (7), a small value of t is needed, but in this case the matrix T tends to become ill-conditioned for a large value of m and deteriorates the truncation errors. An appropriate value for m falls between $n + 1$ and $3n$, and frequently $m = n + 1$ gives a satisfactory result. This can be seen in the following simulation work. This property is quite different from the existing method^{1,2} where at least $2n$ measurement equations are required; the resulting computation involves manipulation with an augmented matrix of a dimension of at least $2n$.

The other point that must be noticed in the present algorithm is identification accuracy, and computational work depends more on the number of sampling data than on the order of the system, as can be seen from Eq. (12). Due to this property, there is no significant difference in identification accuracy for high-order systems as long as the number of sampling data are kept the same. Thus, accuracy comparable to that of low-order systems can be obtained for high-order systems. However, as a system's order increases, the measurement of the complete impulse response matrix becomes difficult, and future work is needed to alleviate this constraint.

Example of Identification

The structural parameters of a spring-mass damper system shown in Fig. 1 are to be identified by simulation study. The parameters m , c , and k are assumed for the purpose of generating the simulated data. Assume that the measurement data is clean and the sampling instants are separated by the same interval T . Define the identification error for the stiff-

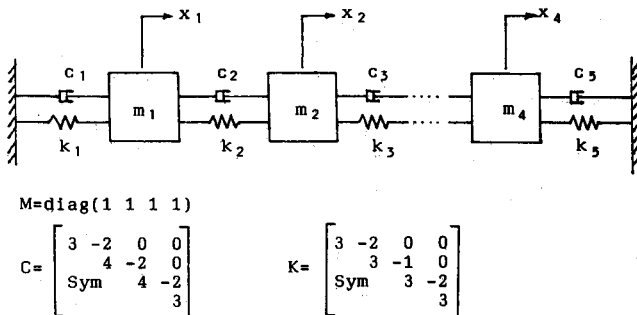


Fig. 1 Spring-mass damper.

ness matrix K by

$$\epsilon_k(m, T) = \max_{i,j} |K_{ij} - K_{ij}(m, T)|$$

where K_{ij} is the element of the exact stiffness matrix K and $K_{ij}(m, T)$ is that computed by the present method with the number of sampling points m and sampling interval T . $\epsilon_M(m, T)$ and $\epsilon_c(m, T)$ are defined in the same way. The simulation results for systems of various orders are depicted in Figs. 2-4. It can be seen from these figures that there exist certain values of m at which the identification error reaches its minimum value. The simulation shows the general tendency for the value of m that minimizes ϵ to fall within the range of

$$n + 1 \leq m \leq 3n$$

For the fourth-order spring-mass damper system, if seven sampling data are used with a sampling interval of 0.02 s, we obtain the following results:

$M = \text{diag}(1.00000 \ 1.00000 \ 1.00000 \ 1.00000)$

$C = \begin{bmatrix} 2.99999 & -1.99999 & -0.00001 & 0.00000 \\ & 3.99999 & -2.00001 & -0.00001 \\ \text{Sym} & & 3.99999 & -1.99999 \\ & & & 2.99999 \end{bmatrix}$

$K = \begin{bmatrix} 2.99970 & -2.00066 & 0.00115 & 0.00042 \\ & 3.00004 & -0.99875 & 0.00115 \\ \text{Sym} & & 3.00004 & -2.00066 \\ & & & 2.99970 \end{bmatrix}$

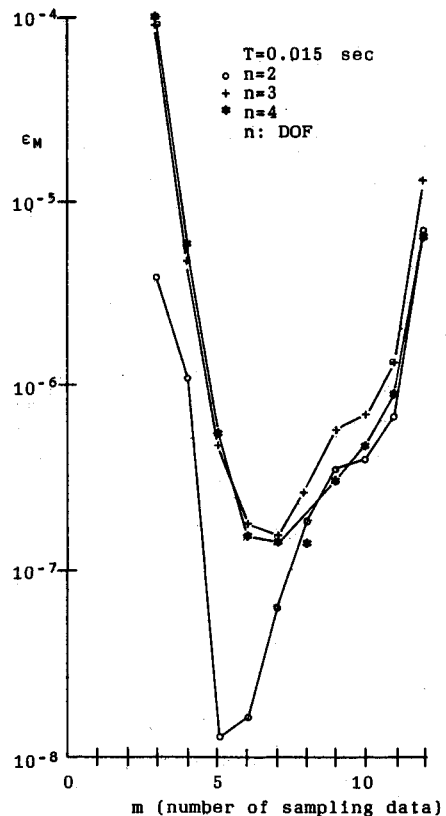


Fig. 2 The identification error of mass coefficients vs number of sampling data.

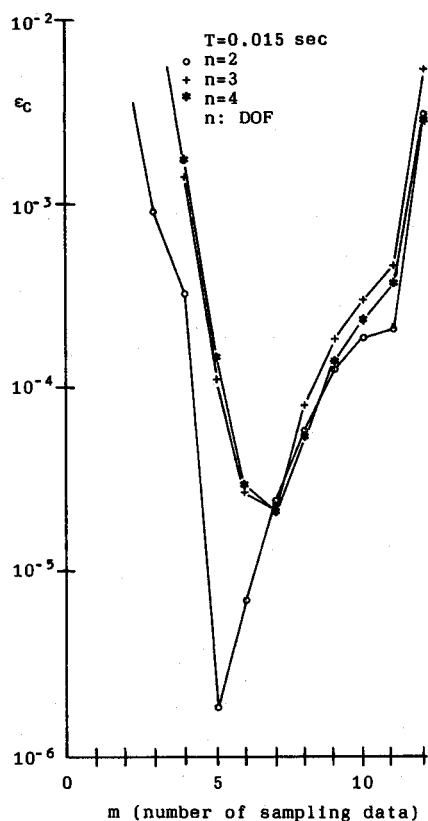


Fig. 3 The identification error of damping coefficients vs number of sampling data.

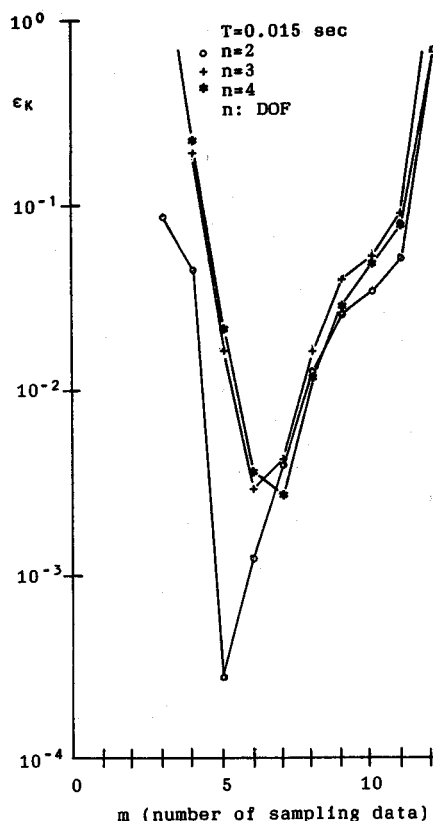


Fig. 4 The identification error of stiffness coefficients vs number of sampling data.

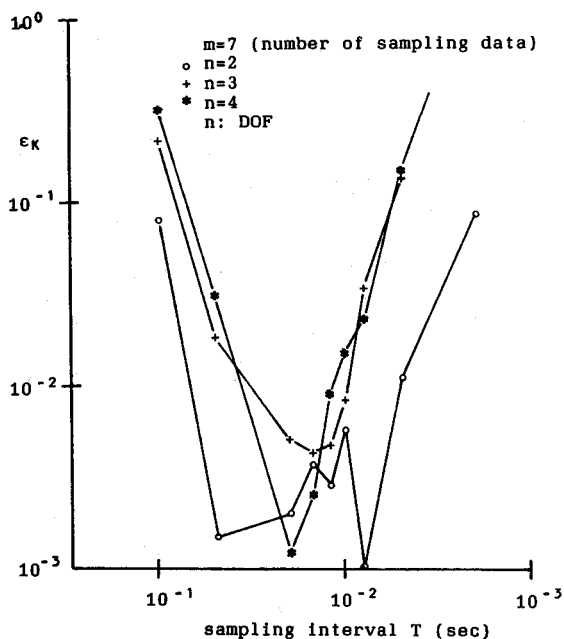


Fig. 5 The identification error of stiffness coefficients vs sampling interval using seven sampling data.

Comparing these simulated values with the assumed coefficients, it can be seen that the maximum relative error of the identified structural parameters does not exceed 0.12%. This accuracy is comparable with that achieved by the combination of the dynamic data systems (DDS) methodology with the finite-element method (FFM).¹ However, the computational work has been significantly reduced in the present method. The variation of the identification error with the sampling interval is depicted in Fig. 5, where the most desirable sampling interval is shown to be between 0.01 and 0.02 s and the minimum relative error is below 0.1%. The simulation results also show that there is no significant difference in the identification error for higher order systems.

Remarks

Using the Hankel parameters obtained from the solution of Eq. (8), we can construct the Hankel matrix

$$\Gamma = \begin{bmatrix} H(1) & H(2) & H(3) & \dots \\ H(2) & H(3) & & \\ \vdots & \vdots & \ddots & \end{bmatrix}$$

From the Kronecker theorem,⁴ we know that the number of nonzero singular values of Γ is equal to the order of the system, and the method of Ref. 5 can be used to determine the order of the system from a finite number of Hankel parameters. The singular-values analysis of the Hankel matrix has also been used as a robust tool for rank characterization⁶⁻⁸ in the presence of noise. The combination of the present method and the techniques of singular-value decomposition and system realization^{7,8} will hopefully give us a useful tool for model reduction and parameter identification from noisy data.

References

- Yuan, J.X. and Wu, X.M., "Identification of the Joint Structural Parameters of Machine Tools by DDS and FFM," *Transactions of the ASME*, Vol. 107, Feb. 1985, pp. 64-69.
- Richardson, M. and Potter, R., "Identification of the Modal Properties of an Elastic Structure from Measured Transfer Function Data," International Instrumentation Symposium, Albuquerque, NM, May 1974.

³Rajaram, S. and Junkins, J.L., "Identification of Vibrating Flexible Structures," *Journal of Guidance and Control*, Vol. 8, July-Aug. 1985, pp. 463-470.

⁴Kailath, T., "Linear Systems," Prentice-Hall, Englewood Cliffs, NJ, 1980.

⁵Young, N.J., "The Singular-Value Decomposition of an Infinite Hankel Matrix," *Linear Algebra and Its Applications*, Vol. 50, 1983, pp. 639-656.

⁶Juang, J.N. and Papa, R.S., "An Eigensystem Realization Algorithm (ERA) for Modal Parameter Identification and Model Reduction," NASA/JPL Workshop on Identification and Control of Flexible Space Structures, San Diego, CA, June 1984.

⁷Kung, S.Y., "A New Identification and Model Reduction Algorithm via Singular Value Decomposition," *Proceedings of the 12th Asilomar Conference on Circuits, Systems, and Computers*, Nov. 1978, pp. 705-714.

⁸Zeiger, H.P. and McEwen, A.J., "Approximate Linear Realization of a Given Dimension via Ho's Algorithm," *IEEE Transactions on Automatic Control*, Vol. AC-19, April 1974, pp. 153.

Improved Method for the Initial Attitude Acquisition Maneuver

John Weissberg* and Keiken Ninomiya†
Institute of Space and Astronautical Science
Tokyo, Japan

Introduction

FOR the initial attitude acquisition maneuver of dual-spin satellites, whose initial spin axis is not that of the maximum moment of inertia, Hubert¹ developed a counterpart to the dual-spin turn of Kaplan and Patterson.² With a passive energy damper to dissipate core energy, the technique uses the momentum wheel to remove the ambiguity in the polarity of the final attitude. In the final attitude, let us call "right-side-up" the case where the wheel's angular momentum vector, as seen from the body frame, is aligned with the inertial one and we will call the opposite case "upside-down." In Hubert's technique, the wheel is maintained so that its angular momentum is always above a certain percentage of the total momentum. This raises the energy level of the upside-down attitude while also destabilizing it. Thus, after all the core energy is dissipated, the final attitude will be the right-side-up one. In this paper, a new technique, along the same lines as Hubert's but without the passive energy damper, is presented. For this new technique, the wheel itself is used as an active core energy dissipator while simultaneously maintaining the conditions necessary to guarantee the final attitude. This eliminates the need for the passive energy damper, saving both weight and expense. The only measurements required for the maneuver are the polarity of a component of the body's angular velocity and the wheel's speed. Both of these can usually be provided by instruments normally onboard.

Analysis

The maneuver is developed for a rigid satellite initially spinning about its axis of minimum moment of inertia. The purpose of the maneuver is to transfer the momentum to a rigid symmetric momentum wheel aligned with the axis of maximum moment of inertia. The principal moments of inertia I_1 , I_2 , and I_3 are defined to include the appropriate components

of the wheel inertia I_w , and satisfy the condition

$$I_3 > I_2 > I_1 \quad (1)$$

In the absence of external torques, the motion is described by the equations

$$\dot{\omega}_1 = -\omega_2 [(I_3 - I_2)\omega_3 + I_w\Omega] / I_1$$

$$\dot{\omega}_2 = \omega_1 [(I_3 - I_1)\omega_3 + I_w\Omega] / I_2 \quad (2)$$

$$\dot{\omega}_3 = -[\omega_1\omega_2(I_2 - I_1) + T] / (I_3 - I_w)$$

$$\dot{\Omega} = T / I_w - \dot{\omega}_3 \quad (3)$$

where ω are the angular velocities, as seen from the body frame, around the respective axes of inertia, and Ω is the angular velocity of the wheel relative to the body. T is the command torque, and friction is neglected here. The core energy E_c is defined as the total energy excluding that part of the energy due solely to the relative motion of the wheel³

$$E_c = \frac{1}{2} (I_1\omega_1^2 + I_2\omega_2^2 + I_3\omega_3^2) \quad (4)$$

The time rate of change for E_c is given by

$$\dot{E}_c = I_1\omega_1\dot{\omega}_1 + I_2\omega_2\dot{\omega}_2 + I_3\omega_3\dot{\omega}_3 \quad (5)$$

Substituting Eqs. (2) and (3) into Eq. (5) yields

$$\dot{E}_c = \frac{-\omega_3}{I_3 - I_w} [\omega_1\omega_2 I_w (I_2 - I_1) + I_3 T] \quad (6)$$

In order to use the wheel successfully as an energy dissipator, we must guarantee that E_c is negative. There are many ways to control the wheel so that this is true. Perhaps the simplest and the easiest to implement is a switched control law of the form

$$T = T_0 \text{sign}(\omega_3) \quad (7)$$

where T_0 is a positive constant and satisfies the following,

$$T_0 > \frac{I_w}{I_3} \frac{h_0^2 (I_2 - I_1)}{2I_1 I_2} \quad (8)$$

and h_0 is the total momentum. We now define the normalized wheel momentum:

$$\Phi = \frac{I_w \Omega}{h_0} \quad (9)$$

The threshold Ψ , defined by Hubert, is

$$\Psi = \frac{I_3 - I_2}{I_2} \quad (10)$$

Provided the condition

$$\Phi \geq \Psi \quad (11)$$

is satisfied during separatrix crossing, then the separatrix leading to the right-side-up attitude will be crossed and the correct final attitude will result. Here we will try to use this same threshold technique to guarantee the final attitude while using the wheel itself as an active energy damper, by implementing a combination of Eqs. (7) and (11).

As a guide to understanding the motion, let us construct the dual-spin polhode curves. If we define h_3^* as the total momentum along the 3 axis,

$$h_3^* = I_3\omega_3 + I_w\Omega \quad (12)$$

Received July 30, 1986; revision received Nov. 7, 1986. Copyright © American Institute of Aeronautics and Astronautics, Inc., 1987. All rights reserved.

*Graduate Student.

†Professor.